ESTIMATED PLASMASPHERE ELECTRON CONTENT AND O⁺/H⁺ TRANSITION HEIGHT DURING THE FEBRUARY 2022 GEOMAGNETIC STORM FROM IRKUTSK IS RADAR DATA

D.S. Khabituev (ORCID)
Institute of Solar-Terrestrial Physics SB RAS,
Irkutsk, Russia, khabituev@iszf.irk.ru

G.A. Zherebtsov (ORCID)
Institute of Solar-Terrestrial Physics SB RAS,
Irkutsk, Russia, gaz@iszf.irk.ru

V.A. Ivonin (ORCID)
Institute of Solar-Terrestrial Physics SB RAS,
Irkutsk, Russia, ivonin1480@mail.iszf.irk.ru

V.P. Lebedev (ORCID)
Institute of Solar-Terrestrial Physics SB RAS,
Irkutsk, Russia, lebedev@mail.iszf.irk.ru

Abstract. We study the topside ionosphere above the $N_\mathrm{m}F2$ ionization maximum and the transition region between the ionosphere and the plasmasphere. We analyze the interaction between the topside ionosphere and the plasmasphere during a strong geomagnetic storm in February 2022, using data from the Irkutsk Incoherent Scatter Radar (IISR) and total electron content data from global navigation satellite systems. To determine the ionosphere and plasmasphere electron contents, an original technique is employed to calculate the integral content of ion density from IISR data, which takes into account the two-component composition of ionospheric plasma. We compare different functions of approximation of the topside ionosphere. The original technique was adjusted for use with IISR N_e data fitted based on the β-Chapman profile. We compare the plasmasphere electron content during quiet and magnetically disturbed days, as well as the dynamics of the O^+/H^+ transition height, which is the upper boundary of the ionosphere and the lower boundary of the plasmasphere.

Keywords: topside ionosphere, plasmasphere, O^+/H^+ transition height, total electron content, incoherent scatter radars.

INTRODUCTION

Interest in the study of the topside ionosphere arose in the 1950s and 1960s, which was associated with the beginning of the space age and the development of new type instruments — incoherent scatter radars. These powerful radars (1–10 MW) are capable of detecting weak backscattering by ionospheric plasma particles. First incoherent scatter radars was built by the USA in the early 1960s and comprised a meridional network of instruments in the Western Hemisphere [Mathews, 2013; Woodman et al., 2019]. Simultaneously with the construction of the first radars, the incoherent scatter theory was actively developed [Evans, 1969; Farley, 1969]. To date, the theory of reconstructing ionospheric parameters from received radio signal has been sufficiently fully developed and allows us to obtain vertical profiles of electron density N_e, electron and ion temperatures, drift velocity, and plasma ion composition. Each incoherent scatter radar has a unique design, which requires an individual approach in developing procedures for reconstructing ionospheric parameters. This also places certain restrictions on the fitting data process. The worldwide network of incoherent scatter radars consists of only 13 facilities, and the Irkutsk Incoherent Scatter Radar (IISR) is the only instrument of this type in Russia. The geographical location of IISR provides coverage of a huge "empty" zone in the north of Eurasia, which makes its data unique and required.

IISR was developed from the military long-range radar station Dnepr, transferred to the Institute of Solar-Terrestrial Physics in the early 1990s [Medvedev, Potekhin, 2019]. When it was redesigned for scientific purposes, a first-generation signal receiving and processing complex was built with software available at that time. The first sessions of regular ionospheric observations with the new complex were run in 1997. The main difference between IISR and other incoherent scatter radars (except for the radar in Jicamarca) is transmission and reception of only linear polarization signals, which produces the Faraday effect in the received signal. The Faraday effect manifests itself as complete fading of the received signal (absence of a signal) when radio wave and receiver polarization planes are orthogonal. Additional difficulties in processing a received signal are created by a low signal-to-noise ratio, which limits the altitude sounding range, especially at low ionospheric electron density. All this often leads to low accuracy in reconstructing ionospheric parameters at large heights, i.e. topside ionosphere heights. Accuracy in reconstructing the electron density profile N_e is inextricably linked to the number of Faraday minima on the received signal power profile. If during high solar activity when the number of minima is high, we confidently reconstruct N_e to 600–800 km, during low solar activity the upper range falls to 400–500 km, i.e. to a height not much higher than the F2-layer maximum. Moreover, the Faraday effect complicates the process of obtaining electron and ion temperatures, drift velocity, and ion plasma composition, which involves considering spectral characteristics of the received signal [Shpynev, 2004] or the autocorrelation function [Tashlykov et al.,

2018]. Unfortunately, comprehensive monitoring of the topside ionosphere with IISR is often limited to reconstructing the electron density profile to the given heights. This work is aimed at exploring the possibility of expanding the diagnostic potential of IISR to high altitudes when combining IISR data with data on total electron content (TEC) from global navigation satellite systems (GNSS). Much attention is also given to the approximation of the topside ionosphere profile by various model profiles and their relevance.

1. TOPSIDE IONOSPHERE PROFILE MODELING

Since the early 2010s, IISR has exploited a new signal recording and processing complex [Medvedev et al., 2004]. To determine the vertical electron density profile, a method based on modeling the total power profile and approximating the measured profile with IISR is adopted. The total power profile is modeled by convoluting the β-Chapman profile with the emitted IISR pulse (the Barker code is employed). Next, the discrepancy functional minimum is found between the measured and model power profiles, and the corresponding Chapman profile becomes a desired profile of the real ionosphere. This method has high speed and accuracy in the vicinity of the F2 layer, yet above the ionization maximum (400–800 km depending on solar activity level) the β-Chapman profile model does not work well.

The electron density based on the β-Chapman profile is calculated by the following formula:

$$N_e(h) =$$
$$= \left(N_mF2 \exp\left[1 - \frac{h - h_mF2}{H} - \exp\left(-\frac{h - h_mF2}{H} \right) \right], \quad (1)$$
$$H = \begin{cases} H_B, h \le h_m \\ H_T, h > H_m \end{cases},$$

where N_e is the electron density of the ionosphere; h is the height measured from the Earth surface; N_mF2 is the F2-layer maximum electron density; h_mF2 is the F2-layer maximum height; H_B is the bottom scale height (bottom side); H_T is the top scale height (top side); . The method of modeling and identifying the coefficients of the model is detailed in [Alsatkin et al.,2020]. As already noted above, this model can be applied to heights no more than 400–600 km (depending on the level of ionosphere electron density). Thus, all information on the behavior of the ionosphere density is omitted above, and it is this region that is most interesting in terms of the coupling between ionosphere/plasmasphere and the magnetosphere, in particular during strong geomagnetic disturbances.

The problem of the discrepancy between the Chapman layer and the measured density profiles has been addressed for quite a long time, and ways to solve it are widely discussed [Stankov, Jakovski, 2006; Reinisch et al., 2007; Kutiev, Marinov, 2007]. Let us look at some of them. To correctly describe N_e in the topside ionosphere and the plasmasphere, a scale height is generally introduced which changes as the mass of dominant ions

decreases and the temperature increases. For example, Marinov et al. [2015] use satellite topside sounding data to determine plasmaspheric and ionospheric scale heights and to study the ratio between these parameters depending on season and magnetic and solar activity levels.

Stankov et al. [2003] have explored the same problem for middle and high latitudes. The authors describe the following method of reconstructing the vertical electron density profile. Data from the DPS-4D ionosonde is applied to the lower ionosphere. The vertical electron density profile of the upper ionosphere is plotted by determining concentrations of O^+ and H^+ and their summation. The ion concentration modeling is based on three analytical models: exponential (2), squared hyperbolic secant (or Epstein layer) (3), and Chapman profile (4):

$$N_i(h) = N_i(h_mF2) \exp\left(-\frac{h - h_mF2}{H_{T_i}} \right), \quad (2)$$

$$N_i(h) = N_i(h_mF2) \operatorname{sech}^2\left(\frac{h - h_mF2}{2H_{T_i}} \right), \quad (3)$$

$$N_i(h) = N_i(h_mF2) \times$$
$$\times \exp\left[\alpha\left(1 - \frac{h - h_mF2}{H_{T_i}} - \exp\left(-\frac{h - h_mF2}{H_{T_i}} \right) \right) \right], \quad (4)$$

where N_i is the concentration of O^+ or H^+; $H_{T_i} = \dfrac{kT_i}{m_i g}$ is the top scale height of O^+ or H^+; α is the shape factor: $\alpha=0.5$ is the α-Chapman profile (the same profile was used to model the atmospheric wind [Kohl, King, 1967]), $\alpha=1$ is the β-Chapman profile. Depending on conditions, one of these three ion density profiles is selected according to TEC, and the corresponding transcendental equation is solved which is derived by equating the O^+ and H^+ concentrations at the O^+/H^+ transition height. Next, the top scale height of O^+ is determined, and the top scale height of H^+ is considered to be 16 times larger.

Firstly, the described method is quite complex in terms of combining various models; secondly, it requires the use of TEC for modeling ion concentrations (to solve equations in order to find the scale height of O^+) from which the electron density is then derived, i.e. the electron density is not directly determined. Furthermore, the developer of this method in a later paper [Verhulst, Stankov, 2017] highlights the need to take into account the diurnal variation of the Sun at different heights of the ionosphere and to differently determine the times of day and night at various points of the Earth surface, which further complicates his method of modeling electron density.

Bilitza et al. [2006], instead of combining a variety of analytical models for various conditions, propose to use not a constant, but a variable top scale height. The most interesting is the approach employed in the development of the model NeQuick 2 [Nava et al., 2008], in which the upper ionosphere is described by the formulas [Pignalberi et al., 2020]

$$N_e(h) = 4N_mF2 \frac{\exp\left(\dfrac{h - h_mF2}{H_T(h)}\right)}{\left(1 + \exp\left(\dfrac{h - h_mF2}{H_T(h)}\right)\right)^2}, \quad (5)$$

$$H_T(h) = H_0\left(1 + \frac{rg(h - h_mF2)}{rH_0 + g(h - h_mF2)}\right), \quad (6)$$

where (5) is the semi-Epstein layer; H_0 is the parameter that depends on N_mF2, h_mF2, F2-layer bottom scale height, and sunspot number; $r=100$; $g=0.125$ is the vertical gradient for H_0 [Leitinger et al., 2005], the denominator in (6) limits the increase in the scale height H_T.

In this work, we have compared vertical TEC calculated by the above models (Formulas (3), (4), (5)), using IISR data, with the following formula:

$$TEC = 10^{-16} \int_0^{20000\,\text{км}} N_e(h)\,dh, \quad (7)$$

where TEC is in TECU (Total Electron Content Unit, 1TECU=10^{16} m^{-2}); $N_e(h)$, in m^{-3}. TEC was obtained from global ionospheric maps (GIM) UQRG, which have a minimum relative error (<20 %) among all currently available GIM [Roma-Dollase et al., 2018]. The main purpose is to select parameters of the model or their combinations such that calculated and measured TEC values coincide.

We have computed vertical TEC from Formula (7) for the aforementioned models (Figure 1). Below h_mF2, integration was always performed using the β-Chapman profile; and above it, in three variants: the β-Chapman profile (blue curve), the α-Chapman profile (green curve), and the semi-Epstein layer (purple curve). Comparison with TEC from GIM UQRG (black curve) shows significant differences between the models. The difference between TEC values from the β-Chapman profile and TEC from GIM UQRG is seen to be 3–4 TECU at night and 5–6 TECU during the day. When using the α-Chapman profile during daylight hours, calculated TEC coincides quite well with TEC from GIM

UQRG, whereas lower values (2–3 TECU) are observed at night. With the semi-Epstein layer, on the contrary, there is a better correspondence between the TEC values at night; and for February 1, 2 and 5, TEC values practically coincide; on February 3 and 4, TEC from GIM UQRG exceeds that from the semi-Epstein layer, which is likely due to the onset of a geomagnetic storm on February 3. During the day, completely unrealistic high values of TEC, calculated from the semi-Epstein layer, are recorded (10–15 TECU higher than TEC from GIM UQRG).

Figure 1 indicates that integral TEC may differ significantly depending on the ionospheric model, i.e. we will significantly underestimate or overestimate real TEC if we choose an improper model. According to the simulation results, the method of reconstructing the electron density profile at IISR with the β-Chapman profile as a basic function significantly underestimates TEC by ~5 TECU, i.e. from 30 to 50 % depending on the date and time of day. If we combine the α-Chapman profile and the semi-Epstein layer to model the upper ionosphere, the error becomes several times smaller. Note that the topside ionosphere makes the main contribution to the difference in TEC when using different models. This time period is a period of low solar activity. Hence, to approximate the electron density of the ionosphere above 400–500 km it is better to employ other ionosphere models than to approximate the entire ionosphere region to 20000 km by the β-Chapman profile [Shpynev, Khabituev, 2014; Khabituev, Shpynev, 2014].

2. SHPYNEV—KHABITUEV METHOD

The Shpynev—Khabituev method (hereinafter referred to as the ShKh method) has been developed for IISR data; it allows us to match the Ne profile with GNSS TEC data, to determine the electron density of the
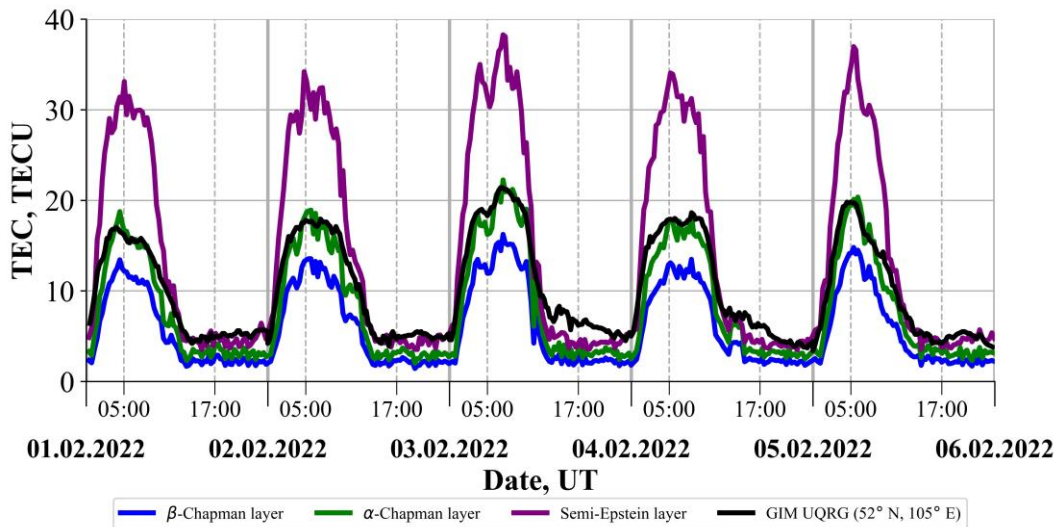

Figure 1. Comparison of TEC from GIM UQRG (black curve) with TEC obtained using various model profiles of N_e for the topside ionosphere: the β- and α-Chapman profiles (blue and green curves) and the semi-Epstein layer (purple curve)

plasmasphere, and the O+/H+ transition height [Shpynev, Khabituev, 2014; Khabituev, Shpynev, 2014]. The method is based on the technology of matching the electron density profile, obtained by IISR, with the integral electron content (i.e., with TEC) to the GNSS orbital height (~20000 km), and a two-component model with a partial concentration of oxygen and hydrogen ions is used to approximate the N_e profile in the topside ionosphere. This method can determine the height at which the dominant component of the ion composition of the ionosphere changes from heavy oxygen ions O^+ to light ions H^+ and He^+ (in the standard version, the method takes into account only H^+), and to estimate the plasmasphere electron content. The critical parameters of the method are the accuracy in determining the vertical electron density profile of the topside ionosphere with IISR and the accuracy in identifying TEC values. The O^+/H^+ transition height is defined as the height of matching of the ionospheric density profile with the integral TEC value. The accuracy in calculating the O^+/H^+ transition height depends on the method of determining the scale height of the topside ionosphere, i.e. how much the electron density decreases above the F2-layer maximum height, and the difference from TEC.

Let us make an important note: the presented method was developed and tested on IISR electron density profiles obtained by a radically different method [Shpynev, 2004] (without β-Chapman profile). This work is the first experience of applying this method to the IISR electron density profiles obtained from the β-Chapman profile [Alsatkin et al., 2020]. The scheme of modeling the profile of the topside ionosphere is presented in Figure 2. The entire modeling region is divided into three areas: TEC1 — from 0 to ~h_mF2, TEC2 — above ~h_mF2 to h_T (where the dominant O^+ ion changes to H^+), and TEC3 — from h_T to the GNSS orbital height (20000 km). The division is made to facilitate the calculation of TEC.

The Faraday effect makes it possible to determine the electron content in TEC1 by summing the number of maxima in power profile of the received signal. Above the peak electron density, the accuracy in detecting Faraday humps decreases and the electron content is found by integrating the reconstructed N_e profile.

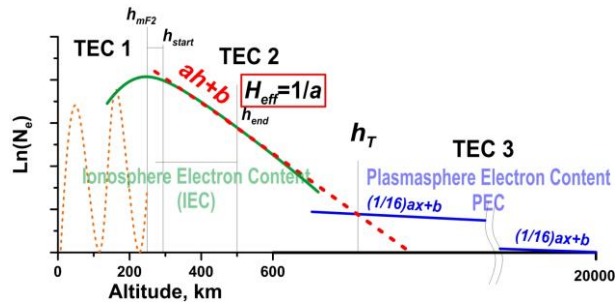In TEC2, the scale height of the topside ionosphere H_{eff} (effective scale height) is defined as the slope of the logarithmic electron density profile $\ln N_e$ since by definition the scale height is the region where the density decreases e times. The vertical profile $N_e(h)$ in the topside ionosphere can be approximated with sufficient accuracy by the expression

$$\ln N_e \cong ah + b, \tag{8}$$

where a and b are the linear regression coefficients of the logarithmic profile of N_e. Then the scale height is

$$H_{eff} = 1/a. \tag{9}$$

This method of calculating the scale height is used in processing experimentally obtained N_e profiles [Shpynev et al., 2010], and H_{eff} may differ significantly from the equilibrium plasma scale height $H_p = kT/(mg)$, where T is the plasma temperature; m is the mass of oxygen ion; g is acceleration of Earth's gravity. It is important in determining H_{eff} to choose the height range $\Delta h = h_{end} - h_{start}$ at which the calculation will be performed. It is reasonable to use a small shift from h_mF2 when calculating H_{eff} in order to avoid distortions caused by the bending of the main F2-layer maximum. The upper limit of the range is found experimentally. Figure 3 plots the dependence of H_{eff} for various altitude ranges on February 1, 2022. It is evident that with an increase in the calculated range the scale height tends to decrease throughout the day, i.e. the slope of the N_e profile increases. The scale height is also seen to be higher at night than during the day. Such dynamics of H_{eff} is often observed in experimental data and is associated with the fact that in the real ionosphere, in addition to temperature and ion mass, dynamic processes affect the scale height. From test calculations it has been found that the altitude range $\Delta h = h_{end} - h_{start} = 240$ km, where $h_{start} = h_m$F2 $+ 60$ km, is optimum for calculating the scale height H_{eff}.

With increasing shift from h_mF2, the accuracy in approximating the density profile increases, but the upper limit of the h_{end} approximation, at which the accuracy of the N_e data decreases, shifts as well. We have therefore chosen an intermediate variant with a shift of 100 samples (1 count = 0.6 km), which allows us to approximate the $\ln N_e$ profile with adequate accuracy. Note that with an altitude range of more than 240 km the error in determining H_{eff} does not exceed 20 % (the difference between blue and brown curves in Figure 3) for local daytime hours (UT+8).
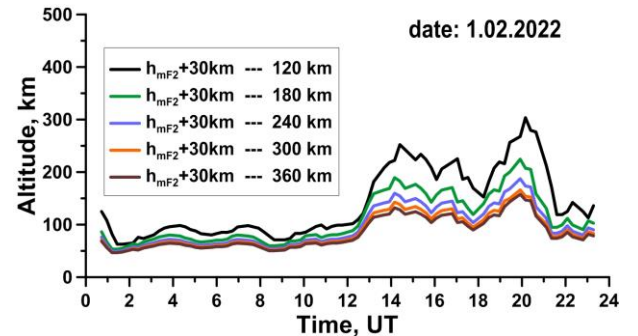

Figure 2. Scheme of modeling the topside ionosphere — plasmasphere and calculating TEC by the Shpynev—Khabituev method

Figure 3. H_{eff} as function of time for different altitude ranges

Ionospheric plasma in the altitude range from h_mF2 to h_T (O^+/H^+ transition heights) consists almost entirely of oxygen ions, hence H_{eff} can be considered an oxygen scale height ($H_{eff} = H_{O^+}$). At high amplitudes (above ~1000 km), hydrogen ions become the dominant component (with an insignificant, no more than 10 %, admixture of helium ions). This fact allows us to use a simple method for calculating the plasmasphere (or hydrogen) scale height:

$$H_{H^+} = 16 H_{O^+}. \quad (10)$$

Assume that at the height of GNSS satellites the plasma density drops to 0 (although this, of course, is not the case, but such an approximation is acceptable when approximating the N_e profile in the ionosphere). Then, knowing the scale heights in various ionosphere and plasmasphere regions, as well as the total integral content (GPS TEC), we can match the two profiles and find the transition height h_T. The final formula for calculating the O^+/H^+ transition height has the form

$$h_T = \frac{1}{a} \ln \left(\frac{a\left(TEC_{GPS} - TEC1\right) + \exp\left(a h_{mF2+60} + b\right)}{\exp b \left(1 + M \dfrac{a}{M} h_{GPS}\right)} \right), \quad (11)$$

where M is the mass factor (the dimensionless coefficient determining the ratio between masses of oxygen and hydrogen ions, i.e. M=16): a, b are the linear regression coefficients of the $\ln N_e$ profile; h_{GPS} is the GPS orbital height (20000 km). A more detailed derivation of the formula is presented in [Shpynev, Khabituev, 2014]. As inferred from (10), the difference between H_{O^+} and H_{H^+} ignores ion and electron temperature variations with height. In the electron density profiles for which the ShKh method was developed, this correction was taken into account during fitting, which led to higher H_{eff} in the daytime. Since the effect of the temperature gradient is ignored in recent IISR data during fitting, the use of the ShKh method requires correction of H_{eff} when calculating h_T.

This procedure can be performed as follows. Introduce a temperature coefficient

$$r_{temp} = T_p\left(h_{end}\right) / T_p\left(h_{start}\right), \quad (12)$$

which takes into account the difference in plasma temperature $T_p = T_i + T_e$ at boundaries of the altitude range Δh. The method allows us to determine T_i and T_e to 450–600 km depending on signal level. If h_{end} is above the temperature detection level, linear extrapolation to this altitude is applied. The r_{temp} coefficient has a diurnal variation with a maximum during the daytime and a minimum at night. Then, the corrected scale height $H_{eff\ cor} = r_{temp} H_{eff}$, and the formula for calculating the transition height is

$$h_T = \frac{r_{temp}}{a} \times$$
$$\times \left(\frac{\dfrac{a}{r_{temp}}\left(TEC_{GPC} - TEC1\right) + \exp\left(\dfrac{a}{r_{temp}} h_{start} + b\right)}{\exp b \left(1 + M r_{temp} - \dfrac{a}{M r_{temp}} h_{GPS}\right)} \right). \quad (13)$$

It is important to emphasize that h_T in the proposed model is determined on the a priori assumption about the difference in the distribution of ionospheric plasma in the lower part of the topside ionosphere and at very high altitudes, i.e. it is the point of matching two density profiles (the topside ionosphere and the plasmasphere) with a predefined difference. The ratio between oxygen and hydrogen ions above and below the transition height is set parametrically.

By determining the transition height h, we can assess the contributions the ionosphere and the plasmasphere make to TEC. TEC1 and TEC2 comprise the Ionosphere Electron Content (IEC), and TEC3 will be called the Plasmasphere Electron Content (PEC); h_T is, in fact, the height of separation between IEC and PEC and defines the lower boundary of the plasmasphere. The question of how to determine the beginning of the plasmasphere: from the height of the beginning of the predominance of light ions or from the free path of particles (i.e. from exobase [Lemaire, Gringauze, 1998]) is debatable and beyond the scope of the study.

3. EXPERIMENT

After adapting the described method for recent IISR data, we have computed the O^+/H^+ transition height from Formula (13), as well as IEC and PEC for geomagnetically quiet and disturbed days, using the February 3–5, 2022 geomagnetic storm as an example. Figure 4 plots the electron content (TEC, IEC, and PEC, top panel), as well as h_T and H_{eff} (middle panels) for February 1–5, 2022. The storm began on February 3, and February 1 and 2 are thought to be magnetically quiet days (background ionosphere). The difference between IEC and TEC on these days is seen to be, on average, 5 TECU during the day and 2.5 TECU at night. Maximum TEC and IEC are observed on February 3, which is associated with an increase in electron density at the beginning of the magnetic storm. After the magnetic storm main phase, significant disturbances occur in the diurnal PEC variations: night PEC values on February 3 are higher than on February 1 and 2, and reach 3–4 TECU; at night on February 4 there are considerable fluctuations in PEC from 0 to 3 TECU.

The difference between universal and local time in Irkutsk is 8 hours, i.e. the local solar noon corresponds to ~05 UT on the plots. An interesting effect is observed before sunrise on February 5 (20–24 UT on February 4) when IEC is compared with the total electron content and PEC drops to zero. The decrease in PEC to zero values coincides with the second minimum of the *Dst* index in the bottom panel of Figure 4. Since the effect may be related to inaccuracy in determining GPS TEC during this period or to the fact that the IISR N_e profile gives overestimated values, additional statistics of such events are required.

Examine now the daily dynamics of h_T and H_{eff} (green and orange curves in Figure 4). During the period of interest, the daily dynamics of the scale height practically does not change: daytime values are 60–80 km and nighttime values are 100–120 km (H_{eff} without regard to r_{temp} here). The transition height h_T exhibits greater vari-
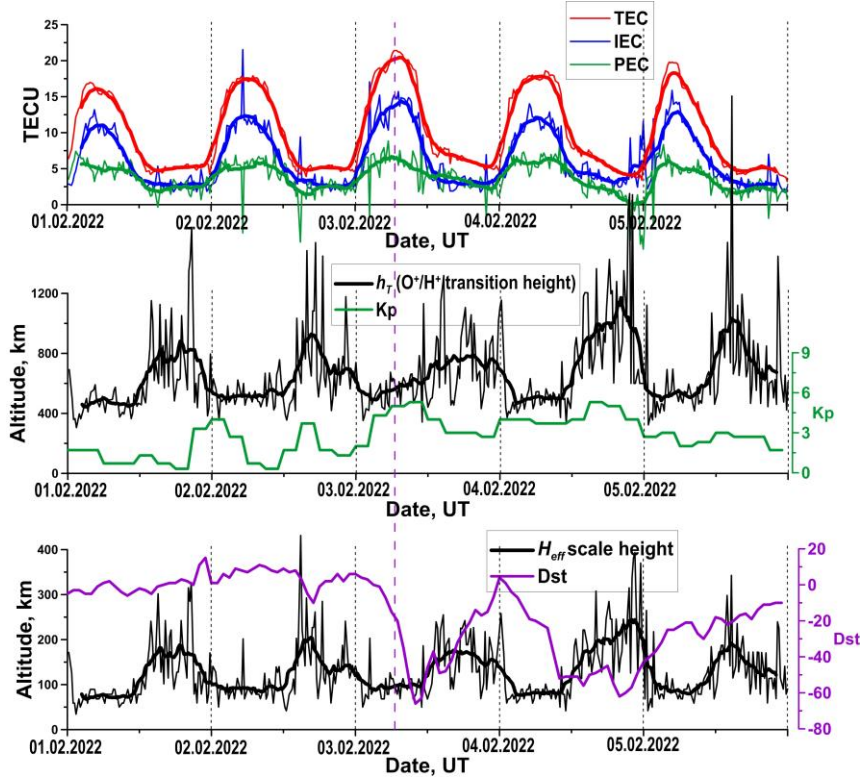
Figure 4. Dynamics of ionosphere and plasmasphere electron contents (top panel), transition height h_T (second panel from above), and scale height H_{eff} (third panel from above) for February 1–5, 2022. Thin lines on the plots indicate obtained values of these parameters; thick curves represent the moving average. The bottom panel displays the geomagnetic (K_p, Dst) and solar activity (F10.7) indices

ability as compared to H_{eff} for all five days of the experiment. On February 01, h_T is as great as 800–1000 km during the daytime with a distinct maximum at noon and decreases to ~600 km at night. Considerable fluctuations in h_T begin in the afternoon of February 2. After the beginning of the magnetic storm main phase on February 3, h_T increases for daytime (1000–1400 km) and for nighttime (700–800 km). Noteworthy is the gradual shift in daily maximum h_T in the dusk on February 4 and 5. Certain values and daily dynamics of h_T generally do not contradict theoretical concepts and the results of self-consistent ionospheric models [Tashchilin, Romanova, 2014; Krinberg, Tashchilin, 1984], yet h_T features lower values during moderate solar activity (F10.7 is shown by red numbers in the bottom panel of Figure 4).We have compared h_T and H_{eff} with data from IRI-2016 [Bilitza et al., 2022] and NeQuick-2. We compared h_T calculated in different ways: from the ion composition profiles of IRI-2016l (the height where the O$^+$ and H$^+$ profiles intersect); by our method from the electron density profiles obtained by IISR, IRI-2016, and NeQuick-2. The input parameters of the models were set with regard to the actual magnetic and solar activity levels. Figure 5 compares the results. The transition height derived from ion composition profiles of IRI-2016 (green curve) has a maximum at 08 UT, and the diurnal amplitude varies from 700 to 1400 km. This height was defined as the height at which $N(O^+)/N_e$=0.5.

The transition height, calculated by the ShKh meth-

od for three different N_e profiles, varies with lower amplitude during the day. Note that for all the three N_e profiles we have used the same data from TEC maps. It is evident that h_T calculated from the N_e profile with the β-Chapman profile (IISR data) coincides quite closely with h_T calculated from the N_e profile of IRI-2016, especially on the first day of the experiment on February 1 (day 32). Nonetheless, the h_T increase from February 1 to February 5 is not observed in both the red and green curves according to IRI-2016 data. The absence of daily values of h_T on the orange curve is due to the fact that NeQuick-2 yields overestimated N_e, and daytime IEC, computed by this model, exceeds GPS TEC, hence the transition height cannot be determined by the described method. The nighttime transition heights according to NeQuick-2 are 800–1000 km and exceed the values obtained from IRI-2016 ionic composition data.

The bottom panel of Figure 5 compares the dynamics of the scale height H_{eff} calculated from the same initial data on N_e. Also shown is H_{eff} computed from the β-Chapman profile, using IISR initial data (blue curve) and H_{eff} corrected for the temperature coefficient r_{temp}. It is obvious that after the correction H_{eff} increases almost twice and daily averages reach ~150 km, which agrees with the values from IRI-2016 and NeQuick-2. Thus, an important conclusion can be drawn that fitting, which includes the β-Chapman profile, yields too low values of the scale height of the topside ionosphere, especially in daytime hours. It is, therefore, necessary to improve the fitting procedure by adding other ionospheric models.
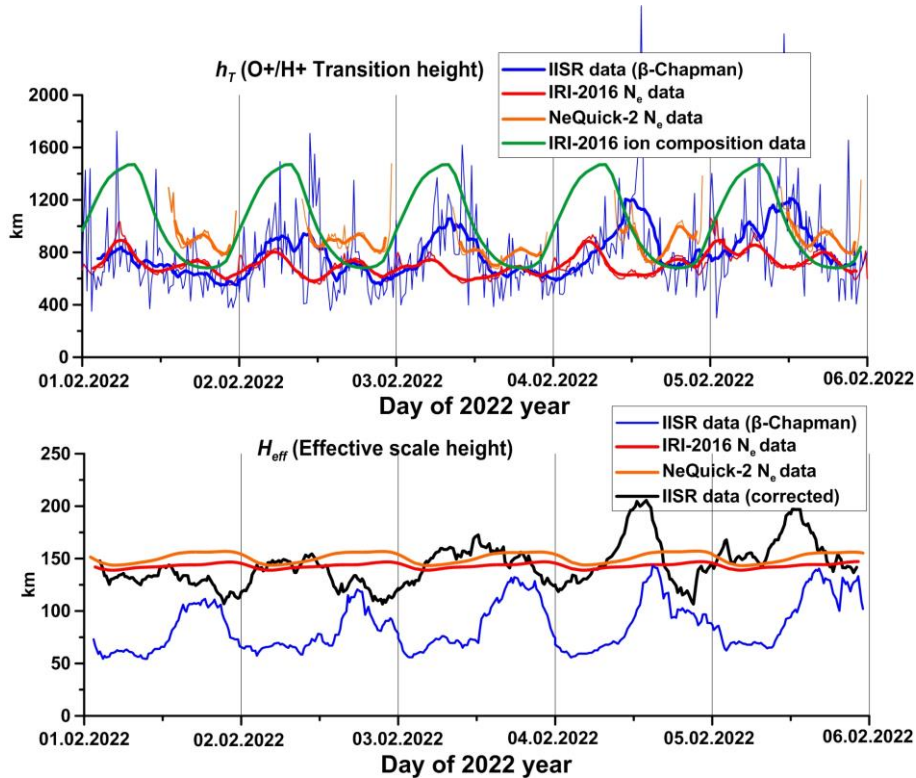
Figure 5. Comparison between dynamics of the transition height h_T (top panel) and the scale height H_{eff} (bottom panel), calculated by the ShKh method from various N_e profiles and IRI-2016 ionic composition data. Thin lines on the plots of the top panel indicate the obtained values of the transition height h_T; the thick curves, the moving average

Examine the profiles of the electron density and the main ionic components obtained by our method for the dayside ionosphere (local noon) at 05.07 UT on February 1 (Figure 6). The N_e profile, reconstructed from the β-Chapman profile (gray dashes), is seen to have a very sharp decrease ($H_{eff} \approx 60$ km). At such a large-scale altitude, N_e decreases to almost 0 already at 600 km. Obviously, if we use such an N_e profile, we cannot match it with the integral value of GPS TEC and adequately estimate the transition height h_T. The blue dashed curve indicates the N_e profile based on the scale height corrected for the temperature coefficient r_{temp}. This correction allows us to fit the O^+ and H^+ profiles into the N_e profile and adequately estimate h_T. For comparison, the plot shows the IRI-2016 electron density profile that has a similar smooth decrease in density in the topside ionosphere. The plot shows that above h_T (the height at which the green and yellow curves intersect) the ShKh method gives higher N_e, which allows us to accumulate several TECU of integral content and correlate it with GPS TEC.

CONCLUSIONS

We have delved into the modeling of the profile of the topside ionosphere, employing different models. We have examined features of reconstruction of the N_e profile with the Irkutsk Incoherent Scattering Radar, using real data obtained during the geomagnetic storm in February 2022. It has been found that the use of the β-Chapman profile as the only model does not allow us to
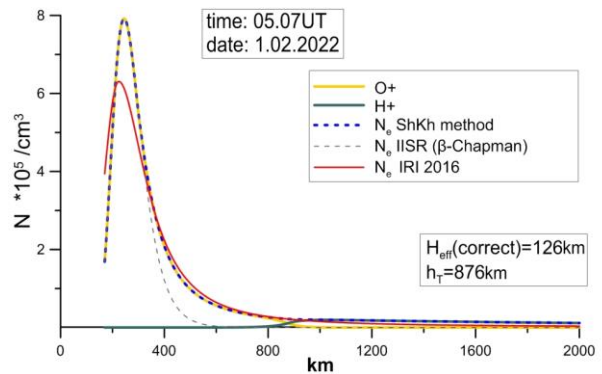

Figure 6. N_e and ion composition profiles for daytime hours on February 1, 2022, derived from IISR data using the ShKh method and the β-Chapman profile, as well as the N_e profile from IRI-2016

match IISR data with GPS TEC. In the first part of the work, we have discussed alternative models (α-Chapman profile, semi-Epstein layer), which, depending on local time, have a closer correspondence with GPS data. We have elaborated the ShKh method, which was previously used to estimate the height of transition from heavy oxygen ions to light hydrogen ions, in order to adapt it for recent IISR data. This method has estimated h_T, as well as ionosphere and plasmasphere integral electron contents during the February 3, 2022 geomagnetic storm. It is shown that after the storm main phase these parameters vary with a high amplitude, which can cause the integral electron content above h_T to drop to zero.

In the future, it is obviously necessary to update the fitting procedure for processing IISR data by increasing the number of fitted models of the topside ionosphere. There is also a need to take into account the temperature coefficient within the fitting procedure to correct the N_e profile at high altitudes. To identify the morphological features of H_{eff} and h_T, we should expand the statistics by processing all available IISR data for various helio- and geomagnetic conditions.

REFERENCES

Alsatkin S.S., Medvedev A.V., Ratovsky K.G. Features of N_e recovery at the Irkutsk Incoherent Scatter Radar. *Solar-Terr. Phys.* 2020, vol. 6, iss. 1, pp. 77–88. DOI: 10.12737/stp-61202009.

Bilitza D., Reinisch B.W., Radicella S.M., Pulinets S., Gulyaeva T., Triskova L. Improvements of the International Reference Ionosphere Model for the topside electron density profile. *Radio Sci.* 2006, vol. 41, iss. 5, pp. 15–22. DOI: 10.1029/ 2005RS003370.

Bilitza D., Pezzopane M., Truhlik V., Altadill D., Reinisch B.W., Pignalberi A. The International Reference Ionosphere Model: A review and description of an ionospheric benchmark. *Rev. Geophys.* 2022, vol. 60, iss. 4, 65 p. DOI: 10.1029/2022RG000792.

Evans J.V. Theory and practice of ionosphere study by Thomson scatter radar. *Proceedings of the IEEE*, 1969, vol. 57, iss. 4, pp. 496–530. DOI: 10.1109/proc.1969.7005.

Farley D.T. Incoherent scatter power measurements; a comparison of various techniques. *Radio Sci.* 1969, vol. 4, iss. 2, pp. 139–142. DOI: 10.1029/RS004i002p00139.

Khabituev D.S., Shpynev B.G. Variations of O^+/H^+ transition height over East Siberia from Irkutsk incoherent scatter data and GPS total electron content. *Sovremennye problemy distantsionnogo zondirovaniya Zemli iz kosmosa* [Current problems in remote sensing of the Earth from space]. 2014, vol. 11, iss. 1, pp. 107–117. (In Russian).

Kohl H., King J.W. Atmospheric winds between 100 and 700 km and their effects on the ionosphere. *J. Atmos. Terr. Phys.* 1967, vol. 29, iss. 9, pp. 1045–1062. DOI: 10.1016/0021-9169(67)90139-0.

Krinberg I.A., Tashchilin A.V. *Ionosfera i plazmosfera Ionosphere and Plasmasphere*. Moscow, Nauka Publ., 1984, 188 p. (In Russian).

Kutiev I., Marinov P. Topside sounder model of scale height and transition height characteristics of the ionosphere. *Adv. Space Res.* 2007, vol. 39, iss. 5, pp. 759–766. DOI: 10.1016/ j.asr.2006.06.013.

Leitinger R., Zhang M.L., Radicella S.M. An improved bottomside for the ionospheric electron density model NeQuick. *Ann. Geophys.* 2005, vol. 48, iss. 3, pp. 525–534. DOI: 10.4401/ag-3217.

Lemaire J. F., Gringauz K.I. The Earth's Plasmasphere. *Cambridge: Cambridge University Press.* 1998, p. 350.

Marinov P., Kutiev I., Belehaki A., Tsagouri I. Modeling the plasmasphere to topside ionosphere scale height ratio. *Journal of Space Weather and Space Climate*, 2015, vol. 5, A27. DOI: 10.1051/swsc/2015028.

Mathews J.D. A short history of geophysical radar at Arecibo Observatory. *History of Geo- and Space Sciences*. 2013, vol. 4, iss. 1, pp. 19–33. DOI: 10.5194/hgss-4-19-2013.

Medvedev A.V., Potekhin A.P. Irkutsk Incoherent Scatter Radar: history, present and future. *History of Geo- and Space Sciences*. 2019, vol. 10, iss. 2, pp. 215–224. DOI: 10.5194/hgss-10-215-2019.

Medvedev A.V., Zavorin A.V., Kushnarev D.S., Shpynev B.G. Modernization of the hardware and software complex of the Irkutsk IS radar. Key elements of a new, multi-channel registration system. *Solnechno-zemnaya fizika* [Solar-Terrestrial Physics], 2004, iss. 5, pp. 107–110. (In Russian).

Nava B., Coïsson P., Radicella S.M. A new version of the NeQuick ionosphere electron density model. *J. Atmos. Solar-Terr. Phys.* 2008, vol. 70, pp. 1856–1862. DOI: 10.1016/j. jastp.2008.01.015.

Pignalberi A., Pezzopane M., Themens D., Haralambous H., Nava B., Coïsson P. On the analytical description of the topside ionosphere by NeQuick: modeling the scale height through COSMIC/FORMOSAT-3 selected data. *IEEE Journal of Selected Topics in Applied Earth Observations and Remote Sensing*. 2020, vol. 13, pp. 1867–1878. DOI: 10.1109/JSTARS.2020.2986683..

Reinisch B.W., Nsumei P., Huang X., Bilitza D. Modeling the F2 topside and plasmasphere for IRI using IMAGE/RPI and ISIS data. *Adv. Space Res.* 2007, vol. 39, iss. 5, pp. 731–738. DOI: 10.1016/j.asr.2006.05.032.

Roma-Dollase D., Hernández-Pajares M., Krankowski A., Kotulak K., Ghoddousi-Fard R., Yuan Y., et al. Consistency of seven different GNSS global ionospheric mapping techniques during one solar cycle. *Journal of Geodesy*. 2018, vol. 92, iss. 4, pp. 691–706. DOI: 10.1007/s00190-017-1088-9.

Shpynev B.G. Incoherent scatter Faraday rotation measurements on a radar with single linear polarization. *Radio Sci.* 2004, vol. 39, iss. 3, 8 p. DOI: 10.1029/2001RS002523.

Shpynev B.G., Khabituev D.S. Estimation of the plasmasphere electron density and O^+/H^+ transition height from Irkutsk incoherent scatter data and GPS total electron content. *J. Atmos. Solar-Terr. Phys.* 2014, vol. 119, pp. 223–228. DOI: 10.1016/j.jastp.2014.01.007.

Shpynev B.G., Zherebtsov G.A., Tashchilin A.V., Khabituyev D.S., Shcherbakov A.A. Analyzing conditions of the mid-latitude outer ionosphere from Irkutsk IS radar measurement data. *Solnechno-zemnaya fizika* [Solar-Terrestrial Physics]. 2010, iss. 16, pp. 3–8. (In Russian).

Stankov S.M., Jakowski N., Heise S., Muhtarov P., Kutiev I., Warnant R. A new method for reconstruction of the vertical electron density distribution in the upper ionosphere and plasmasphere. *J. Geophys. Res.* 2003, vol. 108, iss. A5. pp. 1164–1184. DOI: 10.1029/2002JA009570.

Stankov S.M., Jakovski N. Topside ionospheric scale height analysis and modeling based on radio occultation measurements. *J. Atmos. Solar-Terr. Phys.* 2006, vol. 68, iss. 2, pp. 134–162. DOI: 10.1016/j.jastp.2005.10.003.

Tashlykov V.P., Medvedev A.V., Vasilyev R.V. Backscatter signal model for Irkutsk Incoherent Scatter Radar. *Solar-Terr. Phys*. 2018, vol. 4, iss. 2, pp. 24–32. DOI: 10.12737/stp-42201805.

Tashchilin A.V., Romanova E.B. Modeling the properties of the plasmasphere under quiet and disturbed conditions. *Geomagnetism and Aeronomy*. 2014, vol. 54, iss. 1, pp. 11–19. DOI: 10.1134/S0016793214010150.

Verhulst T.G.W., Stankov S.M. Height-dependent sunrise and sunset: Effects and implications of the varying times of occurrence for local ionospheric processes and modelling. *Adv. Space Res.* 2017, vol. 60, pp. 1797–1806. DOI: 10.1016/ j.asr.2017.05.042.

Woodman R.F., Farley D.T., Balsley B.B., Milla M.A. The early history of the Jicamarca Radio Observatory and the incoherent scatter technique. *History of Geo- and Space Sciences.* 2019, vol. 10, iss. 2, pp. 245–266. DOI: 10.5194/hgss-10-245-2019.

URL: http://ckp-rf.ru/ckp/3056/ (accessed June 20, 2024).
URL: http://ckp-rf.ru/77733/ (accessed June 20, 2024).

How to cite this article
Khabituev D.S., Zherebtsov G.A., Ivonin V.A., Lebedev V.P. Estimated plasmasphere electron content and O+/H+ transition height during the February 2022 geomagnetic storm from Irkutsk IS radar data. *Solar-Terrestrial Physics*. 2024. Vol. 10. Iss. 4. P. 28–36. DOI: 10.12737/stp-104202404.